

# Are Conditional Latent Diffusion Models Effective for Image Restoration?

Yunchen Yuan<sup>1</sup>, Junyuan Xiao<sup>2</sup>, Xinjie Li<sup>3,†</sup>

<sup>1</sup>The Hong Kong Polytechnic University <sup>2</sup>Tsinghua University <sup>3</sup>Pennsylvania State University

## Abstract

*Recent advancements in image restoration increasingly employ conditional latent diffusion models (CLDMs). While these models have demonstrated notable performance improvements in recent years, this work questions their suitability for IR tasks. CLDMs excel in capturing high-level semantic correlations, making them effective for tasks like text-to-image generation with spatial conditioning. However, in IR, where the goal is to enhance image perceptual quality, these models face difficulty of modeling the relationship between degraded images and ground truth images using a low-level representation. To support our claims, we compare state-of-the-art CLDMs with traditional image restoration models through extensive experiments. Results reveal that despite the scaling advantages of CLDMs, they suffer from high distortion and semantic deviation, especially in cases with minimal degradation, where traditional methods outperform them. Additionally, we perform empirical studies to examine the impact of various CLDM design elements on their restoration performance. We hope this finding inspires a reexamination of current CLDM-based IR solutions, opening up more opportunities in this field.*

## 1. Introduction

Image Restoration (IR) is a cornerstone of low-level vision research[4, 7–10, 15, 18, 19, 21, 22, 24, 25, 28], playing a crucial role in improving

the visual quality of images. Traditional IR solutions rely on task-specific knowledge to model degradation and restore images using mathematical modeling and classical signal processing algorithms [2]. Over the past few decades, IR approaches have evolved toward deep learning-based methods, leveraging neural networks to model and enhance the restoration process [17].

In recent years, diffusion models (DMs) have gained prominence as state-of-the-art image generation models, celebrated for their powerful generative capabilities and adaptability [6, 16]. Conditional Latent Diffusion Models (CLDMs) further advance this framework by integrating user-defined image conditions through specialized conditioning modules, enabling precise control in conditional image synthesis [11, 29]. By performing the denoising process in latent space, CLDMs strive to balance computational efficiency with the preservation of fine details.

Recently, Conditional Latent Diffusion Models (CLDMs) have seen a surge in adoption for image restoration (IR) tasks [1, 5, 12, 19, 22, 26, 27, 30]. However, despite these advancements, the effectiveness of CLDMs for IR tasks remains unclear. While these models leverage architectures originally developed for conditional image generation, fundamental differences exist between generative tasks and low-level IR tasks. Generative tasks focus on producing visually plausible outputs conditioned on high-level semantics, whereas IR demands the faithful restoration of perceptual details which often requires precise modeling of low-level representations. This raises a compelling question:

### *Are Conditional Latent Diffusion Models truly effective for image restoration?*

To investigate this question, we conduct comprehensive experiments comparing state-of-the-art CLDM-based image restoration models with traditional deep learning approaches across various tasks. Interestingly, our findings reveal that, despite their scalability advantages, CLDM-based models often fall short in preserving fine-grained details and achieving good distortion metrics. For samples with low degradation levels, where traditional models effectively invert the degradation, CLDM-based approaches still struggle to deliver satisfactory results. Furthermore, CLDMs often introduces semantic deviations in the restored images, which is particularly problematic for restoration tasks requiring precise fidelity. To evaluate the semantic deviation issue, we introduce "Alignment" as a new evaluation aspect, which also facilitates the assessment of real-world blind image restoration.

Furthermore, we perform an in-depth analysis of the CLDM architecture to evaluate how its design elements influence restoration performance. Our empirical experiments reveal that certain architectural components like multi-timesteps and latent space transformation do not enhance restoration performance much but introduce issues such as instability and increased inference time.

Our contributions are as follows:

- To the best of our knowledge, this is the first work to challenge the effectiveness of the booming CLDMs for the image restoration tasks.
- To validate our claims, we compares CLDM-based models with traditional image restoration approaches, we demonstrate that CLDM-based IR solutions exhibit issues like high distortion, semantic deviation, misalignment with resources utilization and model performance.
- We conduct an empirical analysis of critical design components in Conditional Latent Diffusion Models (CLDMs), including latent space representations, noise handling in the diffusion process, and multi-timestep sampling, to evaluate their impact on restoration quality. Our findings reveal that current CLDM-based solutions exhibit architectural misalignments with the ob-

jectives of image restoration tasks.

We hope this work inspires further in-depth exploration of CLDM-based IR solutions, the creation of improved evaluation metrics, and the development of innovative models that transcend current limitations and unlock the full potential of CLDMs in IR’s application.

## 2. Preliminary: Image restoration

Image restoration seeks to recover the ground truth image  $I_x$  from its degraded counterpart  $I_y$ , representing a classic inverse problem. Typically, the degradation process can be expressed as:

$$I_y = \mathcal{D}(I_x; \delta) \downarrow_{\alpha} + \beta \cdot N, \quad (1)$$

where  $\mathcal{D}$  denotes the degradation mapping function,  $I_x$  is the corresponding ground truth image, and  $\delta$  represents the parameters governing the degradation process. The term  $\alpha$  denotes the down-sampling factor, encapsulating the information loss during degradation, while  $N$  represents additional noise, and  $\beta$  is the signal-to-noise ratio.

The inverse of this degradation process is the restoration process, which aims to reconstruct a high-resolution (HR) approximation  $\hat{I}_x$  of the ground truth HR image  $I_x$  from the low-resolution (LR) image  $I_y$ :

$$\hat{I}_x = \mathcal{F}(I_y; \theta), \quad (2)$$

where  $\mathcal{F}$  is the image restoration model, and  $\theta$  represents its parameters.

## 3. CLDM-based IR Pipeline

### 3.1. Initial Restoration Module

In CLDM-based image restoration, a conventional IR model is often employed as the first stage to mitigate degradations such as noise and compression artifacts in low-quality (LQ) images. The initially restored image  $I_{\text{reg}}$  is computed as:

$$I_{\text{reg}} = \mathcal{M}_{\phi}(I_y), \quad (3)$$

where  $\mathcal{M}_{\phi}$  represents the restoration module with parameters  $\phi$ , and  $I_y$  is the LQ input image. The restoration model is typically trained using an  $L_2$  pixel-wise loss, defined as:

$$L_{\text{reg}} = \|I_{\text{reg}} - I_x\|_2^2, \quad (4)$$

where  $I_x$  denotes the high-quality target image.

### 3.2. Perceptual Image Compression

To reduce computational complexity, images are projected from the high-dimensional pixel space into a lower-dimensional latent space using a perceptual compression model, comprising an encoder  $\mathcal{E}$  and a decoder  $\mathcal{D}$ . The encoder maps an image  $x \in \mathbb{R}^{H \times W \times 3}$  to a latent representation  $z = \mathcal{E}(x)$ , while the decoder reconstructs the image as  $\tilde{x} = \mathcal{D}(z)$ . This compression process, which involves downsampling, inevitably introduces information loss, quantified by:

$$\mathcal{L}_{\text{info\_loss}} = \|x - \tilde{x}\|_2^2, \quad (5)$$

### 3.3. Conditioning Modules

In CLDMs, conditioning modules guide the diffusion process using both text and image conditions, which are typically derived from the initially restored image  $I_{\text{reg}}$ .

**Text Conditioning:** A text encoder  $\tau_\theta$  encodes text prompts generated from  $I_{\text{reg}}$  using an image-to-text model  $\mathcal{T}$ :

$$I_{\text{text}} = \mathcal{T}(I_{\text{reg}}), \quad c_t = \tau_\theta(I_{\text{text}}). \quad (6)$$

**Spatial Conditioning:** The latent encoding of the initially restored image  $I_{\text{reg}}$  serves as the image condition:

$$c_f = \mathcal{E}(I_{\text{reg}}), \quad (7)$$

where  $\mathcal{E}$  is the encoder. A connector module further maps features from  $c_f$  to guide the denoising network during the diffusion process. In most CLDM-based IR models, the spatial conditioning module is the primary trainable component.

### 3.4. Training Process

The training process starts with the latent encoding of the ground truth image,  $z_0 = \mathcal{E}(I_x)$ , noise is progressively added to obtain  $z_t$  at timestep  $t$ :

$$z_t = \sqrt{\bar{\alpha}_t} z_0 + \sqrt{1 - \bar{\alpha}_t} \epsilon, \quad (8)$$

where  $\epsilon \sim \mathcal{N}(0, I)$  represents Gaussian noise, and  $\bar{\alpha}_t$  denotes the cumulative product of noise scheduling factors.

The model predicts the noise  $\epsilon_\theta(z_t, t, c_t, c_f)$  through a denoising process. The training objective

minimizes the following loss:

$$\mathcal{L}_{\text{CLDM}} = \mathbb{E}_{t, z_0, \epsilon} [\|\epsilon - \epsilon_\theta(z_t, t, c_t, c_f)\|^2], \quad (9)$$

where  $c_t$  and  $c_f$  are text and spatial conditioning inputs, respectively. To ensure the model learns denoising across different noise levels, timesteps  $t$  are sampled uniformly from  $\{1, \dots, T\}$  during training.

### 3.5. Sampling Process

During sampling, the model iteratively denoises from a random initial latent  $z_T \sim \mathcal{N}(0, I)$ , guided by the conditioning inputs  $c_t$  and  $c_f$ . At each timestep  $t$ , the model predicts  $\epsilon_\theta(z_t, t, c_t, c_f)$  and updates the latent variable as follows:

$$z_{t-1} = \frac{1}{\sqrt{\alpha_t}} \left( z_t - \frac{1 - \alpha_t}{\sqrt{1 - \bar{\alpha}_t}} \epsilon_\theta(z_t, t, c_t, c_f) \right) + \sigma_t \epsilon', \quad (10)$$

where  $\alpha_t$  is the noise schedule factor,  $\sigma_t$  is the standard deviation of the added noise, and  $\epsilon' \sim \mathcal{N}(0, I)$  represents Gaussian noise. After iteratively denoising to  $z_0$ , the final restored image is obtained by decoding the latent variable:

$$\hat{I}_x = \mathcal{D}(z_0), \quad (11)$$

## 4. Issues in CLDM-based IR Solutions

### High Distortion Issue

Classic Image Restoration (CIR) tasks are traditionally defined under constrained settings with simple and well-defined degradation mappings  $\mathcal{D}$ , such as bicubic downsampling. These tasks are typically evaluated using distortion metrics, which quantify the deviation between the restored image and the ground truth, thereby assessing the model's ability to accurately invert the degradation process. The perception-distortion tradeoff, introduced by Blau [3], extends this evaluation by incorporating perception as a metric, emphasizing the naturalness and realism of the restored image.

We compare traditional models and CLDM-based models in two common CIR tasks: super-resolution and deblurring (Fig. 1). While CLDMs demonstrate advantages in perceptual quality, they typically exhibit higher distortion. However, in CIR, distortion serves as the primary evaluation criterion, reflecting a model's ability to accurately

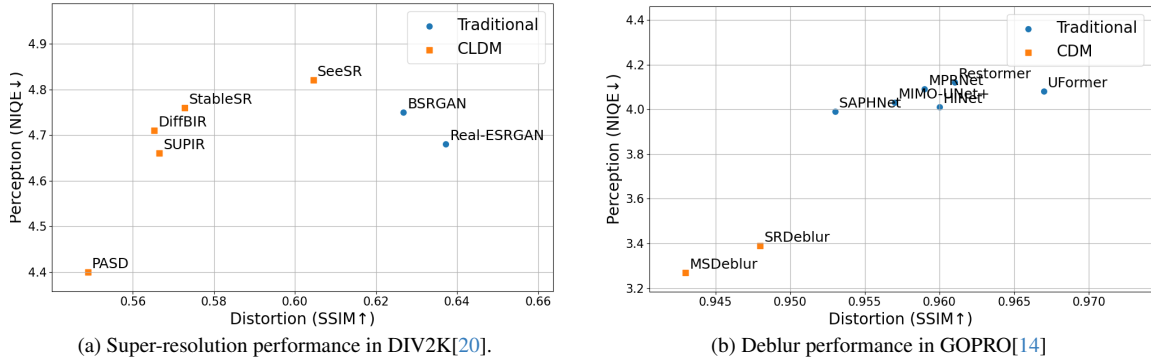


Figure 1. Perception-distortion tradeoff on CIR tasks.

model the restoration process under constrained settings, such as specific tasks and datasets.

Traditional perception-distortion evaluations typically treat the entire validation set uniformly, failing to account for the varying degradation levels present in individual samples. To better characterize this effect, we introduce the information retention rate during the degradation process, defined as:

$$\gamma = \frac{1 - \beta}{\alpha}, \quad (12)$$

where  $\beta$  represents the degradation factor and  $\alpha$  denotes the downsampling rate. As the degradation level increases,  $\gamma$  decreases, making it more challenging to accurately estimate the inverse restoration process.

To explore these dynamics, we evaluate four models on the DIV2K validation dataset [20]: two traditional methods (Real-ESRGAN [23] and Stripformer [21]) and two state-of-the-art CLDM-based methods (DIFFBIR [12] and SUPIR [27]). All models are trained using similar degradation simulation pipelines. The Structural Similarity Index (SSIM) is employed to quantify distortion, while the Natural Image Quality Evaluator (NIQE) [13] is used to assess perceptual quality.

As illustrated in Fig. 2, traditional models excel at low degradation levels, achieving high scores in both distortion and perception metrics. In these scenarios, the degraded images closely resemble their high-quality ground truths, and the upsampling factor is small, making restoration less chal-

lenging. Under such conditions, it is naturally expected that the outputs should not exhibit noticeable distortion, and indeed, traditional methods outperform CLDM-based models.

However, as the degradation level intensifies, restoration becomes significantly more difficult. Traditional models, which rely heavily on explicit degradation detection and compensation, start to produce over-smoothed outputs with visible artifacts. In contrast, CLDM-based models maintain high perceptual quality even under severe degradation. This indicates that diffusion-based methods, while adept at generating realistic details, struggle to ensure fidelity to the original degraded content.

As described in Equation (1), the restoration process involves not only reversing the degradation pattern but also synthesizing fine details required for upsampling. Ultimately, these findings highlight a fundamental trade-off: diffusion-based methods are exceptionally skilled at producing plausible, visually appealing outputs, whereas traditional models are more effective at mitigating degradation and preserving the original image structure, particularly when the degradation level is low.

### Semantic Deviation Issue

We find that Conditional Latent Diffusion Models (CLDMs) often alter semantic details during the restoration process, leading to deviations from the original input semantics (see Fig. 3). Traditional models rely on low-level features such as frequency

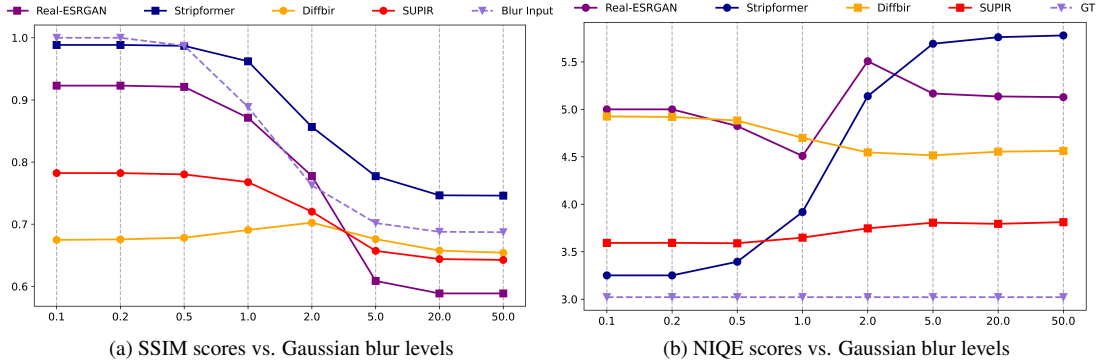


Figure 2. Performance comparison on varying Gaussian blur levels.

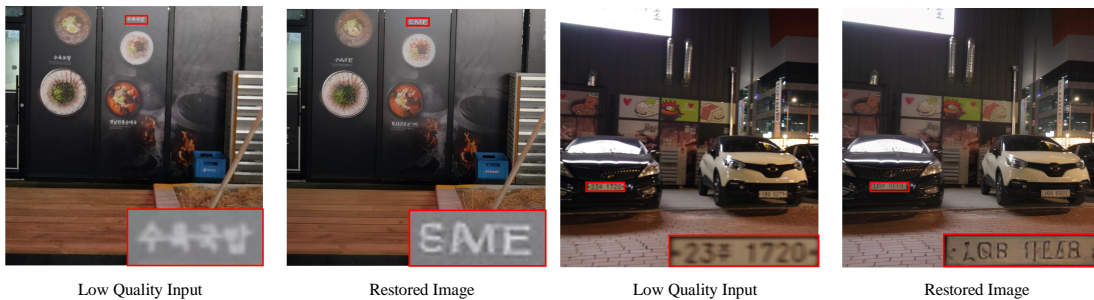


Figure 3. Examples illustrating semantic deviation in CLDM outputs (DIFFBIR).

components and gradients, which inherently lack the capacity to inject new semantic information. In contrast, CLDMs appear to model the restoration process at a semantic level like their generative modeling. As a result, they frequently introduce semantic inconsistencies or "hallucinations," distorting the intended meaning of the original images.

There are currently no established metrics for evaluating semantic deviation in image restoration tasks. To address this limitation, we propose *Alignment* as a new evaluation criterion to measure the semantic consistency between restored images and their degraded inputs at a fine-grained level. Formally, we define Alignment as:

$$\text{Alignment} = \mathcal{S}(I_y, \hat{I}_x), \quad (13)$$

where  $\mathcal{S}(\cdot, \cdot)$  denotes a semantic similarity measure tailored for image restoration.

Measuring Alignment in IR tasks presents notable challenges. Conventional distortion metrics

capture only pixel-level discrepancies, failing to reflect semantic consistency. While semantic encoders such as CLIP and DINOv2 capture high-level concepts, they often lack the fine-grained precision required for detailed semantic comparisons. Moreover, comparing images subjected to different degradation levels introduces additional complexity. Despite these difficulties, we propose a practical, if approximate, approach.

For low-degradation images, we assume that the restored image  $\hat{I}_x$  maintains strong semantic consistency with the ground truth (GT) image  $I_x$ . Under this assumption, we approximate Alignment as:

$$\text{Alignment} \approx \mathcal{S}(I_x, \hat{I}_x). \quad (14)$$

For high-degradation images, direct comparison with the GT image may not accurately reflect semantic alignment due to significant semantic shifts. Instead, we apply the same degradation function  $\mathcal{D}$  used to produce  $I_y$  to the restored image  $\hat{I}_x$ , yield-

Task	Model	DINOv2↓	SSIM↑
SR2	Stripformer	<b>0.1740</b>	<b>0.9149</b>
	Real-ESRGAN	-	-
	DiffBIR	0.5846	0.6987
	SUPIR	0.3839	0.7558
Blur1	Stripformer	<b>0.0953</b>	<b>0.9622</b>
	Real-ESRGAN	0.3166	0.8713
	DiffBIR	0.5971	0.6907
	SUPIR	0.3309	0.7677

(a) Compared with **Ground Truth**

Task	Model	DINOv2↓	SSIM↑
SR4	Stripformer	<b>0.5319</b>	<b>0.9868</b>
	Real-ESRGAN	0.6277	0.9671
	DiffBIR	0.5911	0.9470
	SUPIR	0.5613	0.9553
Blur20	Stripformer	0.6088	<b>0.9761</b>
	Real-ESRGAN	0.6153	0.9393
	DiffBIR	0.6696	0.9536
	SUPIR	<b>0.5476</b>	0.9520

(b) Compared with **Low Quality Input**Table 1. Alignment evaluation. Highlight the best score in **bold**.

ing  $\mathcal{D}(\hat{I}_x)$ :

$$\text{Alignment} \approx S(\mathcal{D}(\hat{I}_x), I_y). \quad (15)$$

This approach enables a comparison under equivalent degradation conditions, though it becomes infeasible if  $\mathcal{D}$  is unknown.

We employed these methods to assess semantic deviations in four tasks: two high-degradation tasks (super-resolution  $\times 4$ , blur  $\sigma = 20$ ) and two low-degradation tasks (super-resolution  $\times 2$ , blur  $\sigma = 1$ ). As shown in Table 1, CLDM-based models fail to maintain semantic consistency with the input, even for low-degradation tasks. While our simple approach leverages existing metrics and is therefore limited, our findings highlight the pressing need for more sophisticated Alignment evaluation methods in image restoration research.

Introducing alignment as a new evaluation aspect helps address the challenges of assessing per-

formance in real-world Blind Image Restoration (BIR). While Classic Image Restoration (CIR) operates within a constrained domain, BIR tackles the restoration of real-world degraded images without constraints on the degradation mapping functions  $\mathcal{D}$ . BIR models are designed to handle complex, multiple, and even mixed types of degradations, demonstrating strong generalization capabilities.

Traditionally, both CIR and BIR have relied on distortion metrics for evaluation. In CIR tasks, the distribution of ground truth images and the degradation processes conform to specific assumptions, making the degradation mapping functions relatively simple and the corresponding inverse process approximations easier to obtain. In contrast, the real-world degradation processes in BIR are more complex, leading to diverse inverse mappings and a larger valid solution domain for the restoration process, where the ground truth image is merely one plausible sample. Consequently, distortion metrics alone are insufficient to comprehensively evaluate restoration quality in BIR tasks. Furthermore, real-world degraded images often lack corresponding ground truth references, adding to the challenge of accurate assessment.

Due to these limitations, some CLDM-based approaches focus on perception evaluation. However, perception is typically assessed using non-reference image quality assessment metrics, which fail to capture the consistency requirements essential in image restoration tasks. In this context, we propose using a combination of alignment and perception, specifically an "alignment-perception tradeoff," as a more effective evaluation framework for BIR tasks.

### Performance vs. Resource Utilization

CLDM-based models exhibit substantial advantages in terms of model scale, as well as the quantity of data employed during both training and pretraining stages. For example, certain models such as SUPIR leverage extensive computational resources and are trained on millions of images, with backbones pre-trained on datasets comprising billions of images. Despite these substantial investments, the resultant performance improvements over traditional models remain limited.

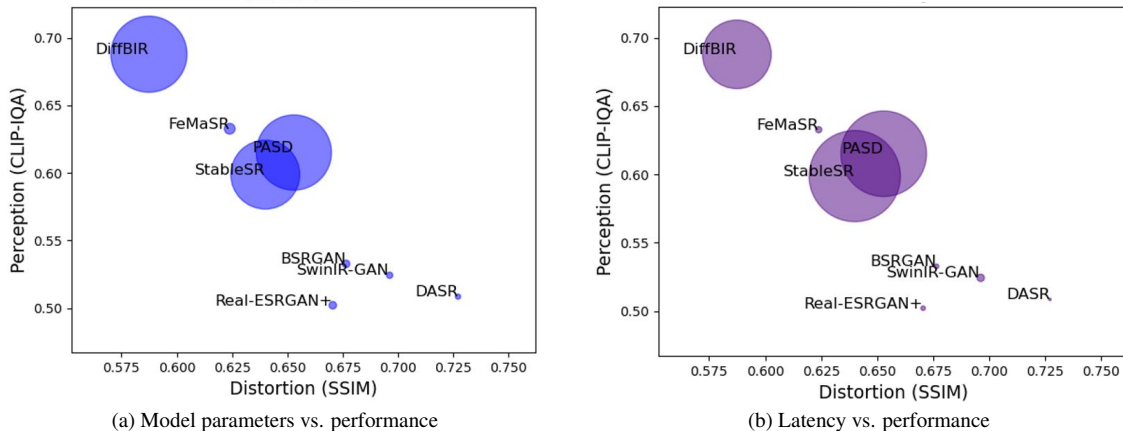


Figure 4. Comparison of performance relative to model parameters and latency.

Moreover, these approaches introduce new issues, including pronounced distortion and semantic deviations, thereby exposing a fundamental discrepancy between resource utilization and achievable performance.

Notably, the application of CLDMs in image restoration tasks directly inherits architectural designs originally developed for conditional image synthesis. However, the intrinsic objectives of these two tasks differ fundamentally. These observations suggest that current CLDM architectures may not be intrinsically aligned with the specific requirements of image restoration and could potentially constrain their capabilities. Furthermore, the observed improvements appear to be largely driven by increased resource allocation rather than the architectural suitability of CLDMs for image restoration tasks.

The related results are shown in Fig. 4.

## 5. More Analysis on CLDMs

### Effectiveness of Latent Space for Image Restoration

Conditional Latent Diffusion Models (CLDMs) restore images through gradual denoising in the latent space. However, the transformation into the latent space introduces downsampling and compression, which can compromise critical perceptual details essential for accurate restoration. While this

	Distortion		Perceptual	
	PSNR $\uparrow$	SSIM $\uparrow$	LPIPS $\downarrow$	NIQE $\downarrow$
GT	-	-	-	3.02
DIFFBIR-VAE	27.72	0.7894	0.0580	3.28
DIFFBIR	25.56	0.7025	0.1421	4.52
SUPIR-VAE	28.68	0.8184	0.0664	3.36
SUPIR	27.27	0.7828	0.0978	3.59

Table 2. Image Quality Metrics Comparison

limitation does not significantly impact generative tasks, as they are not constrained by the precise perceptual fidelity of details, it significantly affects image restoration performance, which heavily relies on low-level perceptual information.

The downsampling inherent in the encoding process imposes a fundamental distortion limit, quantified by the perceptual image compression loss  $\mathcal{L}_{\text{info\_loss}}$  (Eq. 5). Experimental results further confirm that the outputs of CLDMs cannot exceed the quality constraints imposed by this compression (Table 2).

Additionally, we observe that high-frequency details are often lost during the encoding process, and some semantic information is degraded (Fig. 5).

Furthermore, the diffusion loss in CLDMs is



Figure 5. Impact of latent space encoding on image details.

calculated within the latent space, rather than the pixel space. This creates a mismatch between the training objective and the ultimate goal of image restoration tasks.

### Impact of Noise Levels in CLDM Sampling

CLDMs initiate sampling from random Gaussian noise, introducing stochasticity that enhances diversity in generative tasks. However, in image restoration (IR) tasks, diversity is less crucial, as the primary goal is to achieve faithful reconstructions.

We investigate the effect of varying noise levels during sampling by adjusting the starting timestep. Experimental results show that higher noise levels consistently lead to increased distortion without providing notable improvements in perceptual quality, particularly for tasks involving low degradation levels (Fig. 6 in Supplementary Material).

### Effectiveness of Multi-Step Sampling

CLDMs generate images through multi-step denoising, a process critical for modeling complex distributions in generative tasks.

We hypothesize that the modeling of the restoration process is primarily performed by the conditioning module, and the performance of IR is less influenced by the multi-timestep mechanism compared to generative tasks. We conducted experiments with varying numbers of sampling steps. The results indicate that increasing the number of sampling steps does not effectively reduce distortion. (Fig. 7 in Supplementary Material).

To further investigate, we tested one-step prediction and found that the capability of predicting

the ground truth (reflected by distortion metrics) remains nearly the same. Even when starting from pure Gaussian noise, the network achieves its optimal ability to predict the image (Fig. 8 in Supplementary Material).

Additionally, we test the performance at different inference steps, further demonstrating that the multi-timestep sampling process does not improve prediction accuracy but merely enhances image quality (Fig. 9 in Supplementary Material).

## 6. Conclusion

This study questions the effectiveness of emerging CLDM-based solutions for image restoration. By comparing state-of-the-art CLDM models with traditional approaches, we revealed significant limitations of CLDMs, including high distortion, semantic deviations, and a gap between resource utilization and model performance. To address the shortcomings of traditional evaluation metrics in real-world blind image restoration, we proposed a new evaluation aspect—*alignment*, hoping to inspire future more advanced evaluation methods. Our ablation studies indicate that certain design components of CLDMs do not enhance performance in image restoration, highlighting a mismatch between model architecture and task requirements. We anticipate that further analysis of CLDM applications in image restoration will be beneficial and hope that our comprehensive studies will inform and assist future research in this area.

## References

- [1] Yuang Ai, Huaibo Huang, Xiaoqiang Zhou, Jiexiang Wang, and Ran He. Multimodal prompt perceiver: Empower adaptiveness generalizability and fidelity for all-in-one image restoration. In *Proceedings of the IEEE/CVF Conference on Computer Vision and Pattern Recognition*, pages 25432–25444, 2024. 1
- [2] J Amudha, N Pradeepa, and R Sudhakar. A survey on digital image restoration. *Procedia engineering*, 38:2378–2382, 2012. 1
- [3] Yochai Blau and Tomer Michaeli. The perception-distortion tradeoff. In *Proceedings of the IEEE conference on computer vision and pattern recognition*, pages 6228–6237, 2018. 3
- [4] Chaofeng Chen, Xinyu Shi, Yipeng Qin, Xiaoming Li, Xiaoguang Han, Tao Yang, and Shihui Guo. Real-world blind super-resolution via feature matching with implicit high-resolution priors. In *Proceedings of the 30th ACM International Conference on Multimedia*, pages 1329–1338, 2022. 1
- [5] Zheng Chen, Yulun Zhang, Ding Liu, Jinjin Gu, Linghe Kong, Xin Yuan, et al. Hierarchical integration diffusion model for realistic image deblurring. *Advances in neural information processing systems*, 36, 2024. 1
- [6] Jonathan Ho, Ajay Jain, and Pieter Abbeel. Denoising diffusion probabilistic models. *Advances in neural information processing systems*, 33:6840–6851, 2020. 1
- [7] Rusul Sabah Jebur, Mohd Hazli Bin Mohamed Zabil, Dalal Adulmohsin Hammood, and Lim Kok Cheng. A comprehensive review of image denoising in deep learning. *Multimedia Tools and Applications*, 83(20):58181–58199, 2024. 1
- [8] ChuMiao Li. A survey on image deblurring. *arXiv preprint arXiv:2202.07456*, 2022.
- [9] Chongyi Li, Chunle Guo, Linghao Han, Jun Jiang, Ming-Ming Cheng, Jinwei Gu, and Chen Change Loy. Low-light image and video enhancement using deep learning: A survey. *IEEE transactions on pattern analysis and machine intelligence*, 44(12): 9396–9416, 2021.
- [10] Haoying Li, Ziran Zhang, Tingting Jiang, Peng Luo, Huajun Feng, and Zhihai Xu. Real-world deep local motion deblurring, 2023. 1
- [11] Ming Li, Taojiannan Yang, Huaifeng Kuang, Jie Wu, Zhaoning Wang, Xuefeng Xiao, and Chen Chen. Controlnet++: Improving conditional controls with efficient consistency feedback. In *European Conference on Computer Vision*, pages 129–147. Springer, 2025. 1
- [12] Xinqi Lin, Jingwen He, Ziyang Chen, Zhaoyang Lyu, Bo Dai, Fanghua Yu, Wanli Ouyang, Yu Qiao, and Chao Dong. Diffbir: Towards blind image restoration with generative diffusion prior, 2024. 1, 4
- [13] Anish Mittal, Rajiv Soundararajan, and Alan C Bovik. Making a “completely blind” image quality analyzer. *IEEE Signal processing letters*, 20(3): 209–212, 2012. 4
- [14] Seungjun Nah, Tae Hyun Kim, and Kyoung Mu Lee. Deep multi-scale convolutional neural network for dynamic scene deblurring. In *CVPR*, 2017. 4
- [15] Mengwei Ren, Mauricio Delbracio, Hossein Talebi, Guido Gerig, and Peyman Milanfar. Multiscale structure guided diffusion for image deblurring. In *Proceedings of the IEEE/CVF International Conference on Computer Vision*, pages 10721–10733, 2023. 1
- [16] Robin Rombach, Andreas Blattmann, Dominik Lorenz, Patrick Esser, and Björn Ommer. High-resolution image synthesis with latent diffusion models. In *Proceedings of the IEEE/CVF conference on computer vision and pattern recognition*, pages 10684–10695, 2022. 1
- [17] Jingwen Su, Boyan Xu, and Hujun Yin. A survey of deep learning approaches to image restoration. *Neurocomputing*, 487:46–65, 2022. 1
- [18] Xin Tao, Hongyun Gao, Xiaoyong Shen, Jue Wang, and Jiaya Jia. Scale-recurrent network for deep image deblurring. In *Proceedings of the IEEE conference on computer vision and pattern recognition*, pages 8174–8182, 2018. 1
- [19] Yang Tao, Wu Rongyuan, Ren Peiran, Xie Xuan-song, and Zhang Lei. Pixel-aware stable diffusion for realistic image super-resolution and personalized stylization. In *The European Conference on Computer Vision (ECCV) 2024*, 2023. 1
- [20] Radu Timofte, Eirikur Agustsson, Luc Van Gool, Ming-Hsuan Yang, Lei Zhang, Bee Lim, et al. Ntire 2017 challenge on single image super-resolution: Methods and results. In *The IEEE Conference on Computer Vision and Pattern Recognition (CVPR) Workshops*, 2017. 4
- [21] Fu-Jen Tsai, Yan-Tsung Peng, Yen-Yu Lin, Chung-Chi Tsai, and Chia-Wen Lin. Stripformer: Strip

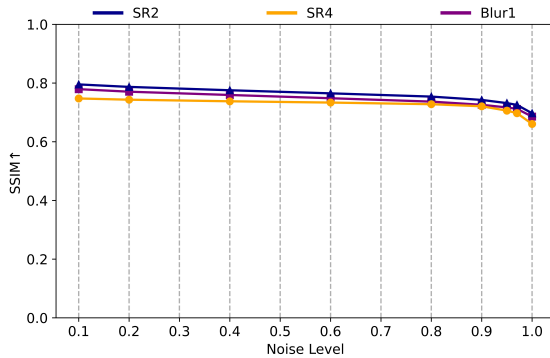
- transformer for fast image deblurring. In *European conference on computer vision*, pages 146–162. Springer, 2022. 1, 4
- [22] Jianyi Wang, Zongsheng Yue, Shangchen Zhou, Kelvin C.K. Chan, and Chen Change Loy. Exploiting diffusion prior for real-world image super-resolution. *International Journal of Computer Vision*, 2024. 1
- [23] Xintao Wang, Liangbin Xie, Chao Dong, and Ying Shan. Real-esrgan: Training real-world blind super-resolution with pure synthetic data. In *International Conference on Computer Vision Workshops (ICCVW)*, 2021. 4
- [24] Zhihao Wang, Jian Chen, and Steven CH Hoi. Deep learning for image super-resolution: A survey. *IEEE transactions on pattern analysis and machine intelligence*, 43(10):3365–3387, 2020. 1
- [25] Jay Whang, Mauricio Delbracio, Hossein Talebi, Chitwan Saharia, Alexandros G Dimakis, and Peyman Milanfar. Deblurring via stochastic refinement. In *Proceedings of the IEEE/CVF Conference on Computer Vision and Pattern Recognition*, pages 16293–16303, 2022. 1
- [26] Bin Xia, Yulun Zhang, Shiyin Wang, Yitong Wang, Xinglong Wu, Yapeng Tian, Wenming Yang, and Luc Van Gool. Diffir: Efficient diffusion model for image restoration. *ICCV*, 2023. 1
- [27] Fanghua Yu, Jinjin Gu, Zheyuan Li, Jinfan Hu, Xiangtao Kong, Xintao Wang, Jingwen He, Yu Qiao, and Chao Dong. Scaling up to excellence: Practicing model scaling for photo-realistic image restoration in the wild, 2024. 1, 4
- [28] Kai Zhang, Jingyun Liang, Luc Van Gool, and Radu Timofte. Designing a practical degradation model for deep blind image super-resolution. In *Proceedings of the IEEE/CVF International Conference on Computer Vision*, pages 4791–4800, 2021. 1
- [29] Lvmin Zhang, Anyi Rao, and Maneesh Agrawala. Adding conditional control to text-to-image diffusion models, 2023. 1
- [30] Yiming Zhang, Zhe Wang, Xinjie Li, Yunchen Yuan, Chengsong Zhang, Xiao Sun, Zhihang Zhong, and Jian Wang. Diffbody: Human body restoration by imagining with generative diffusion prior. In *arXiv preprint arXiv:2404.03642*, 2024. 1

# Are Conditional Latent Diffusion Models Effective for Image Restoration?

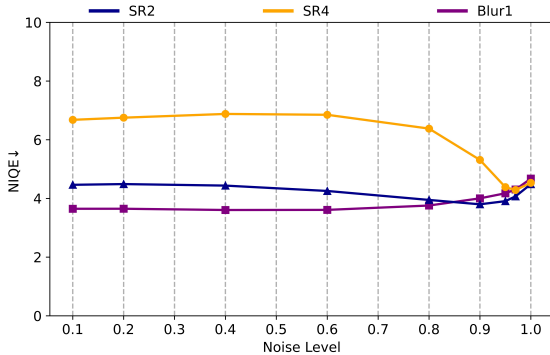
## Supplementary Material

### 7. Overview

Here, we provide Figure 6, 7, 8 and 9 for the main text, which are included here due to space constraints. Note that SR2 refers to 2x super-resolution, SR4 to 4x super-resolution, and Blur1 corresponds to a blur kernel with  $\sigma = 1$ . Additionally, we include further analysis and outline future work in the supplementary material.

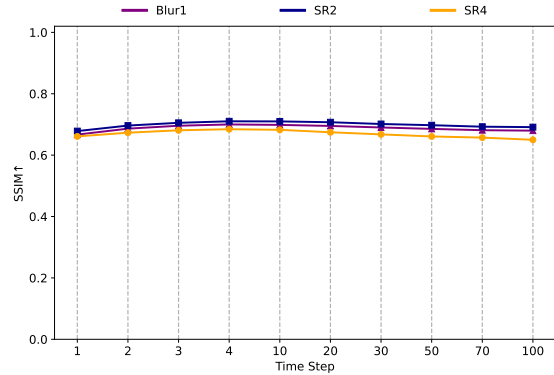


(a) SSIM scores vs. noise levels

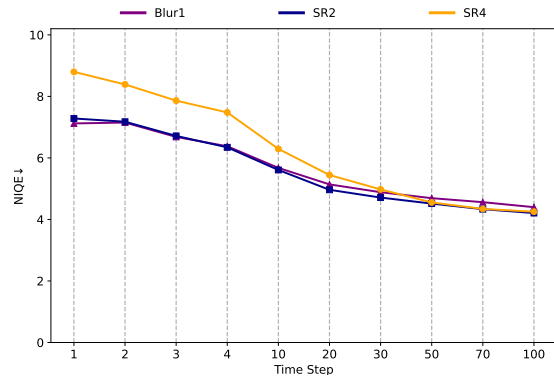


(b) NIQE scores vs. noise levels

Figure 6. Impact of noise levels on distortion (SSIM) and perceptual quality (NIQE).



(a) SSIM for different sampling steps



(b) NIQE for different sampling steps

Figure 7. Impact of sampling steps on distortion (SSIM) and perceptual quality (NIQE).

### 8. More Analysis

#### A. Is DINOv2 Effective for Alignment Evaluation?

To assess the semantic consistency between restored images and their degraded counterparts, we introduce *alignment* as a novel evaluation aspect. Since established metrics for this purpose do not exist, we use differences in embeddings encoded by DINOv2—a visual representation learning model—to estimate semantic deviation. The

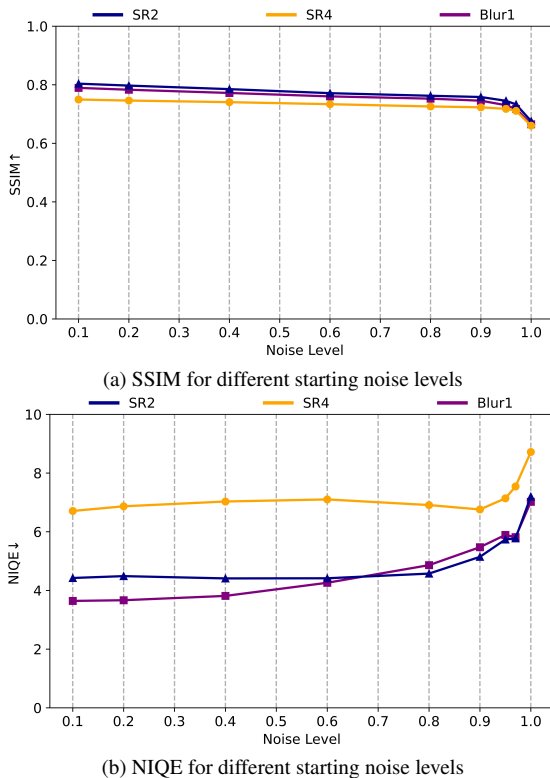


Figure 8. Impact of starting noise levels on one-step prediction.

concept of alignment suggests that the low-quality input and the ground truth image should demonstrate strong semantic correspondence.

As shown in Table 3, calculating the DINOv2 embedding differences between the low-quality input and the ground truth image shows better results compared to other methods, even though distortion metrics fail to capture this improvement. This demonstrates that, while simple, DINOv2 embeddings effectively capture semantic information.

### B. Visual Results for Alignment Evaluation

In this section, we present visual results for alignment evaluation. As illustrated in Figure 10, 11 and 12, the two CLDM-based models consistently exhibit greater semantic deviations in details compared to traditional models across all tasks.

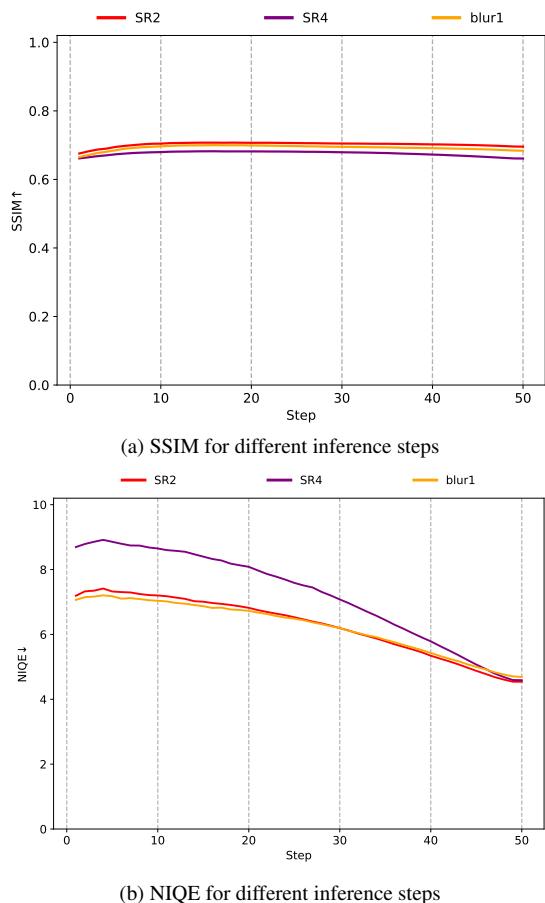


Figure 9. Impact of inference steps on distortion (SSIM) and perceptual quality (NIQE).

Table 3. Alignment evaluation compared with ground truth images.

Task	Model	DINOv2↓	SSIM↑
SR2	LQ	<b>0.0115</b>	0.9080
	DiffBIR	0.5846	0.6987
	Stripformer	0.1740	<b>0.9149</b>
Blur1	LQ	<b>0.0492</b>	0.8886
	DiffBIR	0.5971	0.6907
	Stripformer	0.0953	<b>0.9622</b>

## 9. Future Work

We identify several areas that require further exploration:

- *Comprehensive Evaluation of Models and Tasks.*  
The current analysis is limited to a specific set of models and tasks, which may not yield rigorous or generalizable conclusions. Future work could involve extensive testing on a broader range of models and diverse image restoration (IR) task settings, employing additional evaluation metrics. Furthermore, addressing issues of semantic deviation and model performance across different degradation levels necessitates the development of standardized benchmarking protocols.
- *In-depth Exploration of Influential Factors.*  
This study primarily investigates influential factors such as noise levels, timesteps, and latent space during inference. Future research could explore the impact of various training configurations, including alternative loss functions (e.g., in latent space, pixel space, or feature-based), dynamic noise levels, and timestep control adapted to degradation levels. Additionally, factors like restoration guidance levels, classifier-free guidance, and noise injection during sampling remain unexplored and may significantly affect performance.
- *Development of Alignment Metrics for Image Restoration.*  
This work introduces alignment as a novel evaluation aspect. However, due to the absence of established metrics, it relies on preliminary methods for assessment. Future studies could focus on developing advanced metrics specifically designed to evaluate semantic consistency in IR, thereby providing novel approaches for IR evaluation.
- *Refinement of CLDM Architecture for Image Restoration.*  
Our work shows a misalignment between the existing CLDM architectures and the objectives of IR tasks with various design insights on how different components affect the IR performance. Future work could work on adjusting the CLDM architecture to better fit IR tasks. We also antic-

ipate further research efforts to address existing challenges in CLDM-based IR solutions, such as high distortion, diminished performance on samples with low levels of degradation, and semantic deviations. Given CLDM's substantial advantages in data scalability, model size, and inference efficiency, refining its architecture may unlock significant potential beyond current limitations.

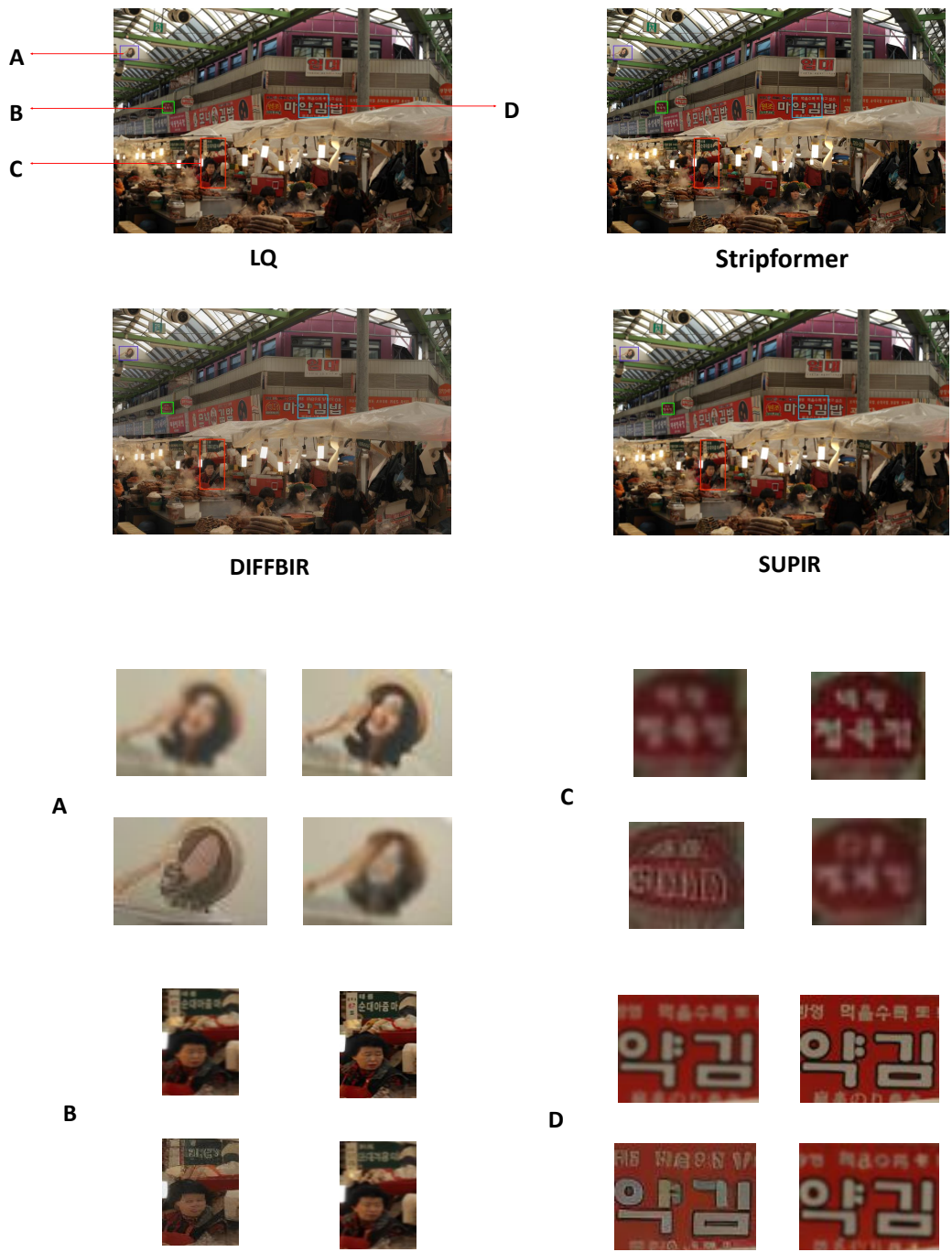


Figure 10. Visual comparison of restored images under the **Blur1** setting. Traditional models retain better semantic consistency, while CLDM-based models exhibit more semantic deviations. Please zoom in for a better comparison.

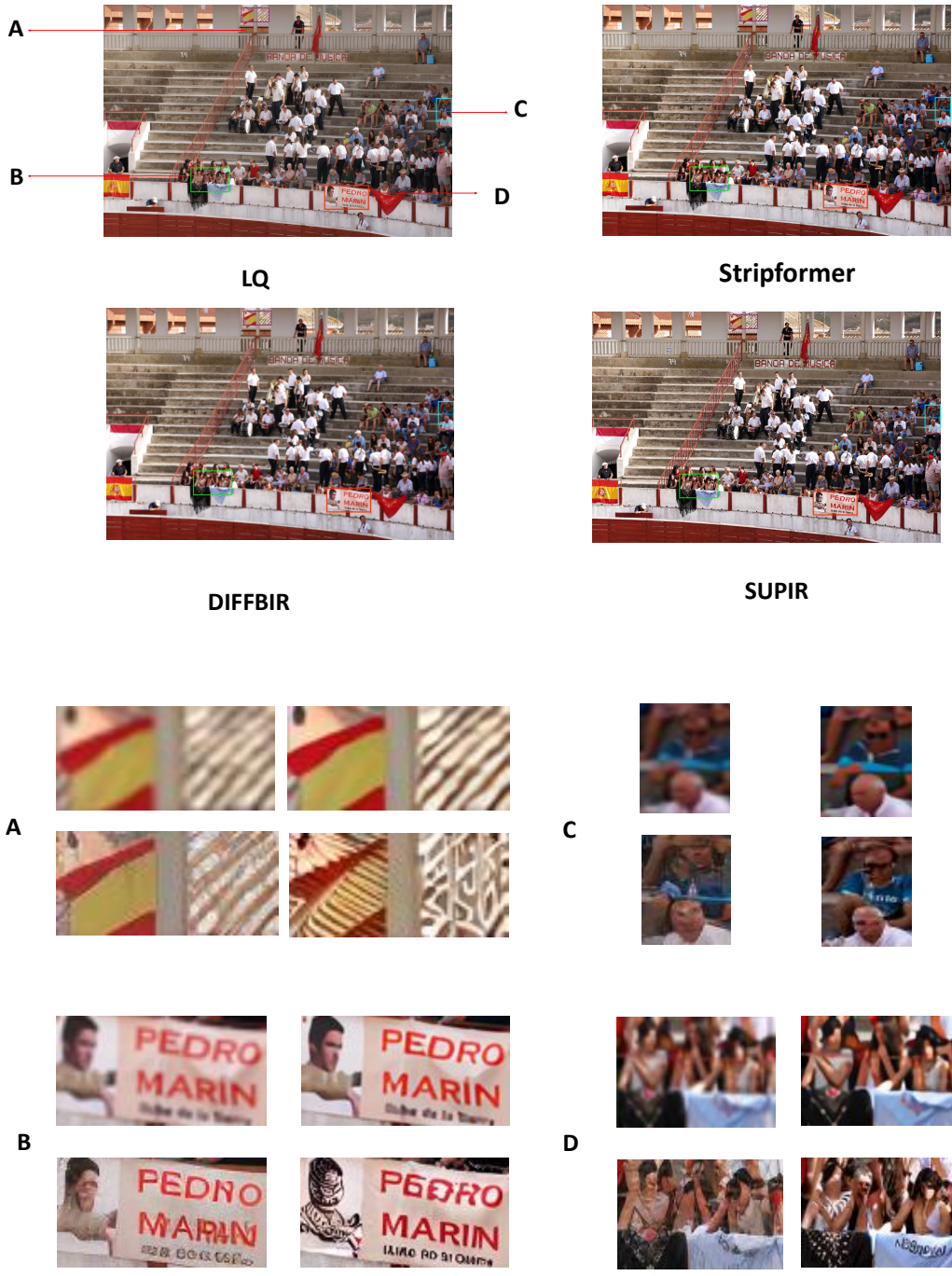


Figure 11. Visual comparison of restored images under the **SR2** setting. The CLDM-based models struggle with fine details, resulting in greater semantic inconsistencies compared to traditional methods. Please zoom in for a better comparison.

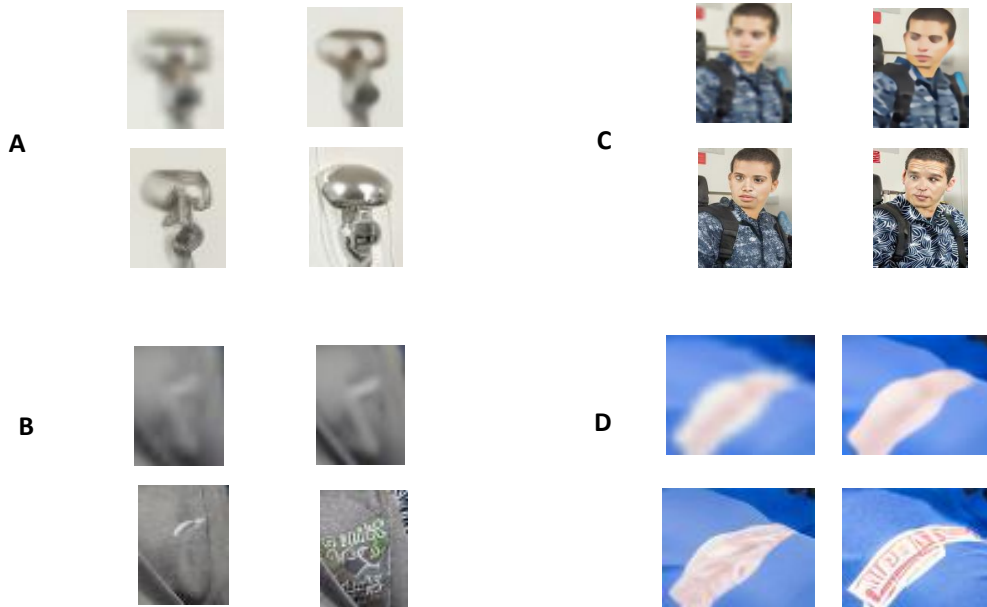
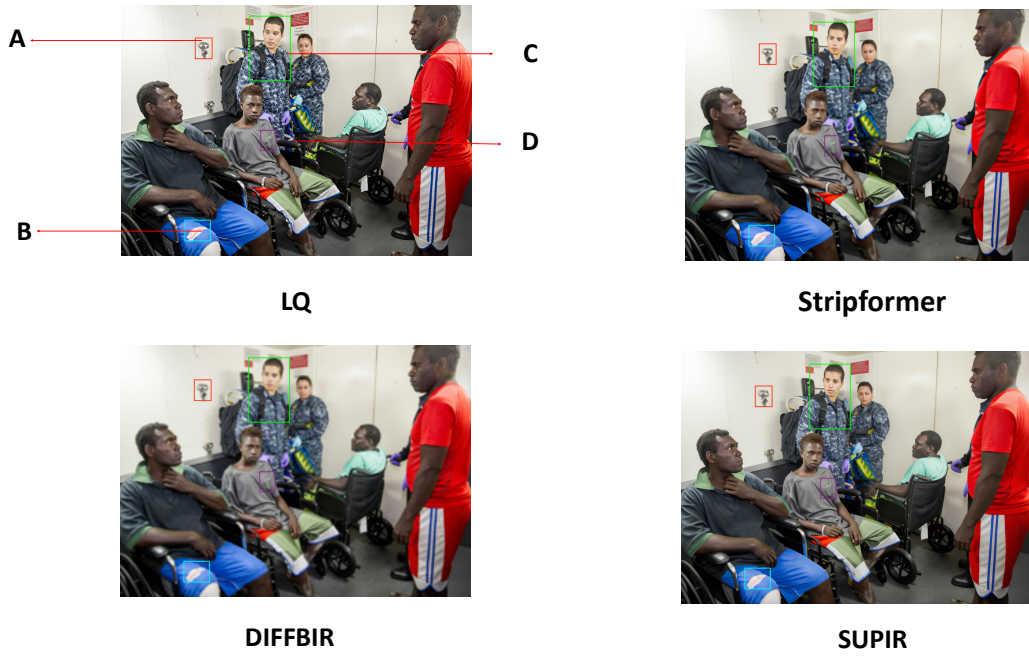


Figure 12. Visual comparison of restored images under the **SR4** setting. Traditional models achieve better alignment, while CLDM-based models introduce noticeable semantic deviations in detailed regions. Please zoom in for a better comparison.